

# Quasinormal modes for the Vaidya metric

Elcio Abdalla\* and Cecilia B. M. H. Chirenti†

*Instituto de Física, Universidade de São Paulo  
C.P. 66318, 05315-970 - São Paulo, SP, Brazil.*

Alberto Saa‡

*Departamento de Matemática Aplicada, UNICAMP  
C.P. 6065, 13083-859 - Campinas, SP, Brazil.*

We consider here scalar and electromagnetic perturbations for the Vaidya metric in double-null coordinates. Such an approach allows one to go a step further in the analysis of quasinormal modes for time-dependent spacetimes. Some recent results are refined, and a new non-stationary behavior corresponding to some sort of inertia for quasinormal modes is identified. Our conclusions can enlighten some aspects of the wave scattering by black holes undergoing some mass accretion processes.

PACS numbers: 04.30.Nk, 04.70.Bw, 04.40.Nr

## I. INTRODUCTION

The quasinormal modes analysis is a paradigm for the study of gravitational excitations of black holes. For a comprehensive review on the vast previous literature, see [1, 2]. The robustness of quasinormal modes (QNM) analysis has been established by considering several kinds of generalizations, as, for instance, relaxing the asymptotic flatness condition[3, 4, 5] or considering time-dependent situations[6, 7, 8]. The case of asymptotic Anti-de-Sitter black holes has deserved special attention due to its relevance to the AdS/CFT conjecture[9, 10, 11, 12, 13, 14, 15, 16, 17, 18, 19, 20, 21].

The analysis of QNM for time-dependent situations is of special physical interest since it is expect that a black hole can enlarge its mass by some accretion process, or even lose mass by some other process, including Hawking radiation. The late time tail for a Klein Gordon field under a time-dependent potential was first considered in [6], where some influence of the temporal dependence of the potential over the characteristic decaying tails was reported. Such a kind of time-dependent potential arises naturally when the Vaidya metric is considered[7, 8]. The Vaidya metric, which in radiation coordinates  $(w, r, \theta, \phi)$  has the form

$$ds^2 = - \left( 1 - \frac{2m(w)}{r} \right) dw^2 + 2cdrdw + r^2 d\Omega^2, \quad (1)$$

where  $d\Omega^2 = d\theta^2 + \sin^2 \theta d\phi^2$ ,  $c = \pm 1$ , is a solution of Einstein's equations with spherical symmetry in the eikonal approximation to a radial flow of unpolarized radiation. For the case of an ingoing radial flow,  $c = 1$  and  $m(w)$  is a monotone increasing mass function in the advanced

time  $w$ , while  $c = -1$  corresponds to an outgoing radial flow, with  $m(w)$  being in this case a monotone decreasing mass function in the retarded time  $w$ . The metric (1) is the starting point for the QNM analysis of varying mass black-holes.

In [8], massless scalar fields were studied on an electrically charged version of the Vaidya metric. Basically, two kinds of continuously varying mass functions were considered:

$$M(w) = \begin{cases} m_1 & w \leq w_1, \\ m_1 f(w) & w_1 \leq w \leq w_2, \\ m_2 & w \geq w_2, \end{cases} \quad (2)$$

with  $f(w) = (1 - \lambda w)$  and  $f(w) = \exp(-\alpha w)$ , called, respectively, linear and exponential models. Generalized tortoise coordinates were introduced, and a standard numerical analysis was done. The conclusion was that, as a first approximation, the QNM for a stationary Reissner-Nordström black hole with mass  $m(w)$  are still valid, as if some stationary adiabatic regime was indeed governing the QNM dynamics for time-dependent spacetimes. In principle, one should not expect such stationary behavior for very rapid varying mass functions, however the analysis of [8] was not able to identify any breaking of such an adiabatic regime. We notice also that both linear and exponential models, inspired by some known exact solutions[22] for which generalized tortoise coordinates could be explicitly constructed, would hardly correspond to physically realistic cases. Both cases have  $C^0$ -class mass functions, implying the existence of some infinitesimal shell distributions of matters for  $w = w_0$  and  $w = w_1$  whose interpretation and role are still unclear.

We attack here the QNM problem by considering the Vaidya metric in double-null coordinates[23]. The main advantage of such approach is the possibility of considering any (monotone) mass function, allowing, for instance, the analysis of smooth mass functions that could correspond to physically more relevant situations, free of obscure infinitesimal matter shells. Furthermore, the use of double-null coordinates has improved considerably the

\*Electronic address: eabdalla@fma.if.usp.br

†Electronic address: cecilia@fma.if.usp.br

‡Electronic address: asaa@ime.unicamp.br

overall precision of the numerical analysis, allowing us to identify the breakdown of the adiabatic regime, characterized by the appearing of a non-stationary inertial effect for the QNM in the case of rapid varying mass functions. Once the stationary regime is reached, the standard QNM results hold, reinforcing, once more, the robustness of the QNM analysis. Our results can be used as a first approximation to describe the propagation of small perturbations around astrophysically realistic situations where black holes undergo some mass accretion processes.

We organize this paper as follows. The next section is devoted to a brief introduction to the semi-analytical approach[23] for the Vaidya metric in double-null coordinates. Section III presents the main issues and results of our numerical analysis. The last section is left to some closing remarks.

## II. THE VAIDYA METRIC IN DOUBLE-NULL COORDINATES

Double-null coordinates are specially suitable for time-evolution problems as the QNM analysis. However, the difficulties of constructing double-null coordinates for non-stationary spacetime are well known. The Vaidya metric is a typical example (see [23] and references therein). Indeed, it is known that the problem of constructing double-null coordinates for generic mass functions is not analytical soluble in general[22]. The semi-analytical approach proposed in [23] is the starting point for our analysis here. It consists, basically, in considering the Vaidya metric in double-null coordinates *ab initio*, avoiding the need of constructing any coordinate transformation. The spherically symmetric line element in double-null coordinates is

$$ds^2 = -2f(u, v)du dv + r^2(u, v)d\Omega^2, \quad (3)$$

where  $f(u, v)$  and  $r(u, v)$  are smooth non vanishing functions. The energy-momentum tensor of a unidirectional radial flow of unpolarized radiation in the eikonal approximation is given by

$$T_{ab} = \frac{1}{8\pi}h(u, v)k_a k_b, \quad (4)$$

where  $k_a$  is a radial null vector. The Einstein's equations for the case of a flow in the  $v$ -direction can then be reduced to the following set of equations[22, 23]

$$f(u, v) = 2B(v)\partial_u r(u, v), \quad (5)$$

$$\partial_v r(u, v) = -B(v)\left(1 - \frac{2m(v)}{r(u, v)}\right), \quad (6)$$

$$h(u, v) = -4\frac{B(v)m'(v)}{r^2(u, v)}, \quad (7)$$

where  $B(v)$  and  $m(v)$  are arbitrary functions obeying, according to the weak energy condition,

$$B(v)m'(v) \leq 0. \quad (8)$$

The solution of (5)-(7) will correspond to the Vaidya metric in double-null coordinates, as one can interpret from (3) and (4). For  $m'(v) \neq 0$ , the choice

$$B = -\frac{1}{2}\text{sign}(m') \quad (9)$$

allows one to interpret  $m(v)$  as the mass of the solution and  $v$  as the proper time as measured in the rest frame at infinity for the asymptotically flat case[22, 23]. Note that if the weak energy condition (8) holds, the function  $m(v)$  is monotone, implying that the radial flow must be ingoing or outgoing for all  $v$ . It is not possible, for instance, to have "oscillating" mass functions  $m(v)$ .

The semi-analytical approach of [23] consists in a strategy to construct numerically the functions  $f(u, v)$ ,  $r(u, v)$  and  $h(u, v)$  from the Eq. (5)-(7), and to infer the underlying causal structure. Eq. (6) along  $u$  constant is a first order ordinary differential equation in  $v$ . One can evaluate the function  $r(u, v)$  in any point by solving the  $v$ -initial value problem knowing  $r(u, v_0)$ . The trivial example of Minkowski spacetime ( $m = 0$ ), for instance, can be obtained by choosing  $r(u, 0) = u/2$ [23]. Once we have  $r(u, v)$ , we can evaluate  $f(u, v)$  and  $h(u, v)$  from (5) and (7). Further details of the method can be found in [23]. We consider here the following smooth mass function

$$m(v) = m_1 + \frac{m_2 - m_1}{2} [1 + \tanh \rho(v - v_1)] \quad (10)$$

where  $\rho$  and  $v_1$  are also constant parameters. For sake of comparison with the results of [8], we also consider a linear model. Fig. 1 depicts the causal structure corresponding to the hyperbolic mass function (10) obtained

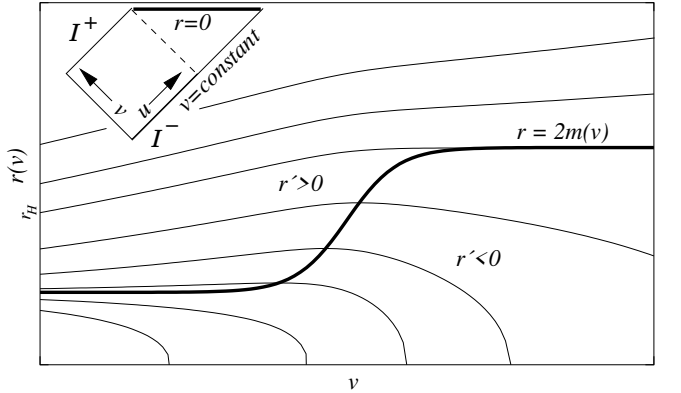


FIG. 1: Lines of constant  $u$  for the solution of (6) with the hyperbolic mass function (10), with  $m_2 > m_1$  and  $\rho > 0$ . All solutions in the region below the line  $r = 2m(v)$  (the apparent horizon) have  $r' < 0$ . Any solution that enters into this region will reach the singularity at  $r = 0$  with finite  $v$ . On the other hand, solutions confined to the  $r' > 0$  region always escape from the singularity and reach  $\mathcal{I}^+$ . In the present case, there exists an event horizon (the dashed line on the inserted conformal diagram) close to the solutions  $r_H(v)$ .

from the semi-analytical approach. For positive  $\rho$  and  $m_2 > m_1$ , for instance, it represents a black hole with

mass  $m_1$  receiving a radial flux of radiation and, consequently, enlarging continuously its mass until reaching  $m_2$ . The choice of the initial condition for solving (6) is a rather subtle issue[23]. For our purposes here, we note only that demanding  $\partial_u r(u, v_0) \neq 0$  is sufficient to guarantee that, for any  $m(v)$ , the underlying spacetime causal structure does not depend on the initial condition  $r(u, v_0)$ . For constant  $m$  and  $B = -1/2$ , Eq. (6) can be easily integrated, leading to

$$r(u, v) + 2m \ln |r(u, v) - 2m| - \frac{v}{2} = P(u), \quad (11)$$

where  $P(u)$  is an arbitrary function of  $u$ . It is also possible to solve Eq. (6) analytically for the linear and exponential mass functions[22]. Eq. (11) is our reference to choose the initial conditions  $r(u, v_0)$ .

### III. SCALAR AND ELECTROMAGNETIC PERTURBATIONS

In the coordinate system (3), for any desired form of the mass function  $m(v)$ , the equations for scalar and electromagnetic perturbations can be easily put in the form[2]

$$\frac{\partial^2 \psi}{\partial u \partial v} + V(u, v) f(u, v) \psi = 0, \quad (12)$$

where the potential  $V(u, v)$  is given by

$$V(u, v) = \frac{\ell(\ell + 1)}{2r^2(u, v)} + \sigma \frac{m(v)}{r^3(u, v)}, \quad (13)$$

where  $\sigma = 1$  and  $\sigma = 0$  correspond, respectively, to the scalar and to the electromagnetic cases. For a given mass function  $m(v)$ , one first evaluates the function  $f(u, v)$  and  $r(u, v)$  with the semi-analytical approach of the previous section, and then the characteristic problem corresponding to (12) can be solved with the usual second order algorithm[2], where the initial data are specified along the two null surfaces  $u = u_0$  and  $v = v_0$ . Since the basic aspects of the field decay are independent of the initial conditions (this fact is confirmed by our simulations), we use the Gaussian initial condition

$$\psi(u = u_0, v) = \exp \left[ -\frac{(v - v_c)^2}{2\sigma^2} \right], \quad (14)$$

and  $\psi(u, v = v_0) = \text{const}$ . Our typical numerical grid is large enough to assure that we can set effectively this last constant to zero. After the integration is completed, the values  $\psi(u_{max}, v)$  are extracted, where  $u_{max}$  is the maximum value of  $u$  on the numerical grid. Taking sufficiently large  $u_{max}$ , we have good approximations for the wave function at the event horizon. Figure 2 presents an example of  $\psi(u_{max}, v)$  data for a hyperbolic increasing mass function and its comparison with the case of a Schwarzschild black hole. Similar results hold if we

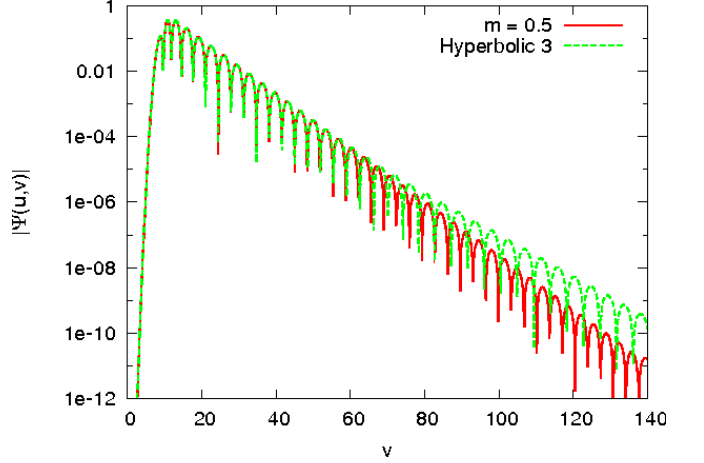


FIG. 2: Values of the electromagnetic perturbations  $\psi(u_{max}, v)$  with  $\ell = 2$  for a Schwarzschild black hole with mass  $m = 0.5$  and for the Vaidya metric with the hyperbolic mass function (10), where  $v_1 = 75$ ,  $\rho = 0.08$ ,  $m_1 = 0.5$ , and  $m_2 = 0.65$  (Hyperbolic 3). One can clearly appreciate, for the time-dependent case, the slowing down of the oscillation frequency and damping taking place after  $v_1$ .

extract the data for other values of  $u$ . All the analysis presented here corresponds to the data extracted on the horizon  $u_{max}$ .

From the function  $\psi(u_{max}, v)$ , one can infer the characteristic frequencies  $\omega$  of the damped oscillating modes. Since the frequencies  $\omega$  are themselves time-dependent (see Fig. 2), for a given  $v$ ,  $\omega(v)$  is determined locally by a non-linear  $\chi^2$ -fitting by using some damped cycles of  $\psi$  around  $v$ . We perform an exhaustive numerical anal-

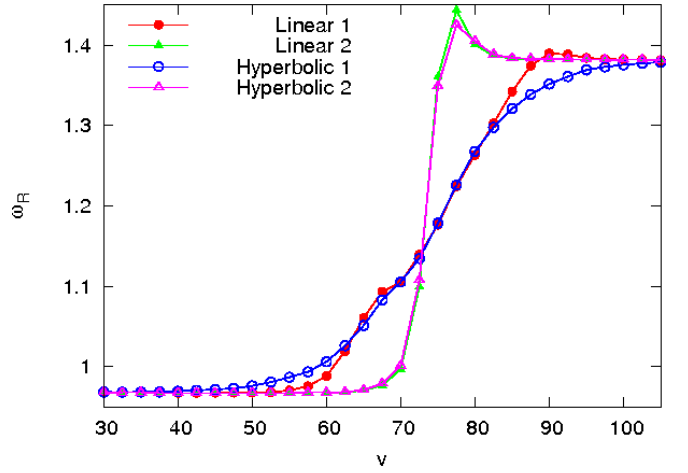


FIG. 3: The real part ( $\omega_R$ ) of the frequency for scalar perturbations with  $\ell = 2$  as function of  $v$  for decreasing linear and hyperbolic mass functions. For all the cases,  $m_1 = 0.5$  and  $m_2 = 0.35$ . Linear 1:  $v_1 = 60$ ,  $v_2 = 90$ . Linear 2:  $v_1 = 74.5$ ,  $v_2 = 75.5$ . Hyperbolic 1:  $v_1 = 75$ ,  $\rho = 0.08$ . Hyperbolic 2:  $v_1 = 75$ ,  $\rho = 0.8$ .

ysis for many different mass functions  $m(v)$ . Figures 3

and 4 present the real part ( $\omega_R$ ) of the frequency of some perturbations as function of  $v$ . Figures 3 and 4 correspond, respectively, to some decreasing and increasing mass functions. They are typical for all values of  $\ell$ , all kinds of perturbations (scalar and electromagnetic) and different initial conditions. The imaginary part  $\omega_I$  exhibits similar time-dependence, although its values are typically known with lower precision than  $\omega_R$ .

Let us take for a close analysis, for instance, the case of decreasing  $m(v)$  (Fig. 3). For the rapid varying cases (Linear 2 and Hyperbolic 2), one clearly sees the inertial effect for  $\omega_R$  near  $v = 75$ . The function  $\omega_R(v)$  does not follow the track corresponding to  $m^{-1}(v)$ , as one would expect for a stationary adiabatic regime, and as it really does for the Hyperbolic 1 case. After the rapid increasing phase,  $\omega_R$  acts as it would have some intrinsic inertia, reaching a maximum value that is bigger than  $\omega_R(\infty)$ , implying the relaxation corresponding to the region with  $\omega'_R(v) < 0$  for  $v > 75$ . We also notice that, for the rapid varying case, one could not detect sensible differences between the smooth hyperbolic case and the  $C^0$  linear one. Nevertheless, one can see that the slower linear case (Linear 1) exhibits some inertial effects close the the second matching point of  $m(v)$ . In all other regions, it follows the track corresponding to  $m^{-1}(v)$ . No appreciable difference in the transients of scalar and electromagnetic perturbations was detected. As we have already mentioned, such transient inertial behavior passed unnoticed by the QNM analysis in radiation coordinates performed in [8]. Analogous conclusions hold for the case of increasing  $m(v)$  (Fig. 4). In fact, since the increasing

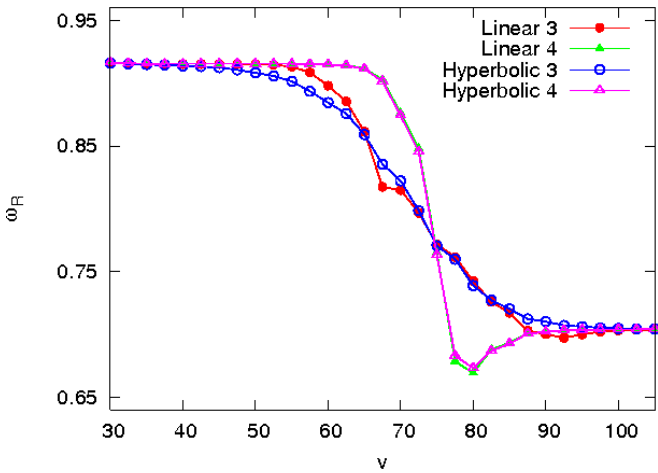


FIG. 4: The real part ( $\omega_R$ ) of the frequency for electromagnetic perturbations with  $\ell = 2$  as function of  $v$  for increasing linear and hyperbolic mass functions. For all the cases,  $m_1 = 0.5$  and  $m_2 = 0.65$ . Linear 3:  $v_1 = 60$ ,  $v_2 = 90$ . Linear 4:  $v_1 = 74.5$ ,  $v_2 = 75.5$ . Hyperbolic 3:  $v_1 = 75$ ,  $\rho = 0.08$ . Hyperbolic 4:  $v_1 = 75$ ,  $\rho = 0.8$ .

ing mass functions considered here can be obtained from the decreasing ones by a time-reversal  $m(v) \rightarrow m(-v)$ , the underlying causal structures are equivalent[23], and

the corresponding QNM are also related. Under a time-reversal, the graph of  $\omega_R$  (and of  $\omega_I$ ) must be reflected on a horizontal axis.

#### IV. FINAL REMARKS

All situations we considered in the present work involve mass functions corresponding to an initial black hole with mass  $m_1$  undergoing some accretion/losing mass process and ending with a mass  $m_2$ . Such an “asymptotic Schwarzschild” choice assures us that the spacetime has the usual black hole causal structure for  $v \rightarrow \pm\infty$  and, consequently, that QNM can be defined in the usual way and that the corresponding frequencies can be properly compared. For all the cases considered, the inertial transients dissipate away and  $\omega(v)$  tends to follow the track of  $m^{-1}(v)$  rather quickly, rendering the robustness of the numerical QNM analysis. The integration in double-null coordinates has turned out to be much more efficient than the integration in radiation coordinates[8], allowing us to reach the precision necessary to unveil the reported non-stationary behavior with quite modest computational resources.

Although the typical astrophysical situations of mass accretion for black holes will hardly keep spherical symmetry intact during intermediate stages, our results can be used as a first approximation for the scattering by this sources since, as it is well known, after the transient phases, the system should accommodate itself in a stationary spherical symmetric configuration. The evaporation by Hawking radiation could indeed be considered as a physically genuine process where the black hole mass decreases and spherical symmetry is maintained. Our approach can be applied for this case, with some crucial remarks about the causal structure of the spacetime left behind after the evaporation[24].

We finish by noticing, as it is well known, that the damped oscillations correspond to an intermediate phase in the wave scattering by asymptotic flat black holes. The very last final phase corresponds, indeed, to a power law decay. In the problems considered here, the power law tail typically appears for large values of  $v$  for which the QNM already settled down in the stationary phase, with no trace from the transients. We do not detect, in this case, any influence of the time-dependence of the potential in these tails. There is no contradiction with the results reported in [6]. This is a consequence of our choice of “asymptotic Schwarzschild” mass functions, for which the corresponding potential has no resemblance with those ones considered in [6].

#### Acknowledgments

The author are grateful to FAPESP and CNPq for the financial support.

---

[1] H.P. Nollert, *Class. Quantum Grav.* **16**, R159 (1999).

[2] K.D. Kokkotas and B.G. Schmidt, *Living Rev. Rel.* **2**, 2 (1999), [arXiv:gr-qc/9909058].

[3] P.R. Brady, C.M. Chambers, W. Krivan, and P. Laguna, *Phys. Rev.* **D55**, 7538(1997), [arXiv:gr-qc/9611056]; P.R. Brady, C.M. Chambers, W.G. Laarakkers and E. Poisson, *Phys. Rev.* **D60**, 064003 (1999), [arXiv:gr-qc/9902010].

[4] C. Molina, D. Giugno E. Abdalla and A. Saa, *Phys. Rev.* **D69**, 104013 (2004), [arXiv:gr-qc/0309079].

[5] D.P. Du, B. Wang and R.K. Su, *Phys. Rev.* **D70**, 064024 (2004), [arXiv:hep-th/0404047]; E. Abdalla, B. Wang, A. Lima-Santos and W.G. Qiu, *Phys. Lett.* **538B**, 435 (2000), [arXiv:hep-th/0204030]; E. Abdalla, K.H.C. Castello-Brando and A. Lima-Santos, *Phys. Rev.* **D66**, 104018 (2002), [arXiv:hep-th/0208065].

[6] S. Hod, *Phys. Rev.* **D66**, 024001 (2002), [arXiv:gr-qc/0201017].

[7] L.H. Xue, Z.X. Shen, B. Wang and R.K. Su, *Mod. Phys. Lett.* **A19**, 239 (2004), [arXiv:gr-qc/0304109].

[8] C.G. Shao, B. Wang, E. Abdalla, and R.K. Su, *Phys. Rev.* **D71**, 044003 (2005), [arXiv:gr-qc/0410025].

[9] J.S.F. Chan and R.B. Mann, *Phys. Rev.* **D55**, 7546 (1997), [arXiv:gr-qc/9612026]; *Phys. Rev.* **D59**, 064025 (1999).

[10] V. Cardoso and J.P.S. Lemos, *Phys. Rev.* **D63**, 124015 (2001), [arXiv:gr-qc/0101052].

[11] G.T. Horowitz and V.E. Hubeny, *Phys. Rev.* **D62**, 024027 (2000), [arXiv:hep-th/9909056].

[12] B. Wang, C.Y. Lin and E. Abdalla, *Phys. Lett.* **481B**, 79 (2000), [arXiv:hep-th/0003295].

[13] B. Wang, C. Molina and E. Abdalla, *Phys. Rev.* **D63**, 084001 (2001), [arXiv:hep-th/0005143].

[14] V. Cardoso and J.P.S. Lemos, *Phys. Rev.* **D64**, 084017 (2001), [arXiv:gr-qc/0105103]; *Class. Quantum. Grav.* **18**, 5257 (2001), [arXiv:gr-qc/0107098].

[15] E. Berti and K.D. Kokkotas, *Phys. Rev.* **D67**, 064020 (2003), [arXiv:gr-qc/0301052].

[16] R.A. Konoplya, *Phys. Rev.* **D66**, 044009 (2002), [arXiv:hep-th/0205142].

[17] D. Birmingham, I. Sachs, S.N. Solodukhin, *Phys. Rev. Lett.* **88**, 151301 (2002), [arXiv:hep-th/0112055]; D. Birmingham, *Phys. Rev.* **D64**, 064024 (2001), [arXiv:hep-th/0101194].

[18] J.M. Zhu, B. Wang and E. Abdalla, *Phys. Rev.* **D63**, 124004 (2001), [arXiv:hep-th/0101133]; B. Wang, E. Abdalla and R.B. Mann, *Phys. Rev.* **D65**, 084006 (2002), [arXiv:hep-th/0107243]; B. Wang, C.Y. Lin and C. Molina, *Phys. Rev.* **D70**, 064025 (2004), [arXiv:hep-th/0407024].

[19] S. Musiri and G. Siopsis, *Phys. Lett.* **576B**, 309 (2003), [arXiv:hep-th/0308196]; R. Aros, C. Martinez, R. Troncoso and J. Zanelli, *Phys. Rev.* **D67**, 044014 (2003), [arXiv:hep-th/0211024]; A. Nunez and A.O. Starinets, *Phys. Rev.* **D67**, 124013 (2003), [arXiv:hep-th/0302026]; E. Winstanley, *Phys. Rev.* **D64**, 104010 (2001), [arXiv:gr-qc/0106032].

[20] V. Cardoso and J.P.S. Lemos, *Phys. Rev.* **D67**, 084020 (2003), [arXiv:gr-qc/0301078].

[21] V. Cardoso, R. Konoplya and J.P.S. Lemos, *Phys. Rev.* **D68**, 044024 (2003), [arXiv:gr-qc/0305037].

[22] B. Waugh and K. Lake, *Phys. Rev.* **D34**, 2978 (1986).

[23] F. Girotto and A. Saa, *Phys. Rev.* **D70**, 084014 (2004), [arXiv:gr-qc/0406067].

[24] E. Abdalla, C. B. M. H. Chirenti, and A. Saa, to appear.